Article

Combined Impacts of ENSO and IOD on Streamflow: A Case Study of the Jinsha River Basin, China

Wenhao Jia [1,2], Yawen Wu [3,*], Sen Wang [1,2], Mufeng Chen [4] and Xia Liu [1]

[1] Pearl River Water Resources Research Institute, Guangzhou 510611, China
[2] Key Laboratory of the Pearl River Estuary Regulation and Protection of Ministry of Water Resources, Guangzhou 510611, China
[3] College of Water Conservancy and Civil Engineering, Shandong Agricultural University, Taian 271018, China
[4] Department of Aquatic Ecosystem Analysis and Management, Helmholtz Centre for Environmental Research—UFZ, 39104 Leipzig, Germany
[*] Correspondence: yawen.wu@sdau.edu.cn

Abstract: This study investigated the combined impacts of the El Niño–Southern Oscillation (ENSO) and the Indian Ocean Dipole (IOD) on streamflow under four scenarios: neutral, pure ENSO, pure IOD, and a combination of ENSO and IOD. The Jinsha River Basin (JRB), at the head of the Yangtze River, was used as a case study. By using statistical methods such as coherent wavelet analysis (WTC), we are committed to studying what kind of impact the IOD will have, the difference in impact between ENSO and IOD at different stages, and the difference in impact between ENSO and IOD on the mean and extreme values of runoff, compared with traditional single ENSO event, to provide support for water resource management, especially for reservoir operation. The key results are as follows. (a) Both ENSO and IOD events affect annual and seasonal streamflow in the JRB. (b) The impact of pure IOD events on annual streamflow in the JRB was twice as great as that of pure ENSO events in developing years, whereas the opposite was true in decaying years. (c) The combined impact of ENSO and IOD led to a higher streamflow maximum than the annual or seasonal average streamflow. Conversely, their impact on the streamflow minima was less than 10% during both developing and decaying years, except at Zhimenda Station. (d) Overall, water shortages could be more serious in developing years than in neutral years, and much more attention should be given to flooding control in decaying years. These results can be used as a reference for water resource management concerning agricultural planning and ecological protection in the JRB.

Keywords: ENSO; IOD; streamflow; precipitation; Jinsha River Basin

1. Introduction

From a resource management perspective, streamflow contributes to the sustainable availability of water, which is vital for human health, economic activities, ecosystem functions, as well as geophysical processes. The Jinsha River is located in southwestern China and is widely known as the "water tower" of the Yangtze River. Additionally, the Jinsha River Basin (JRB) is the water source for the South-to-North Water Transfer West Route Project [1], and it is also an important part of the "West-to-East Power Transmission Project" [2]. The streamflow of JRB plays an important role in the regional water cycle and influences energy balance, climate change, and ecosystem processes, as well as China's economic and social development [3]. However, tropical climate drivers, including the El Niño-Southern Oscillation (ENSO) and the Indian Ocean Dipole (IOD), whose influence extends up to the mid-latitudes, can induce changes in stream flow amounts and characteristics, thereby generating new challenges for water resource management [4].

The repeated cycle of ENSO events, which is a relatively well-documented phenomenon [5–7], varies in length from 2–7 years [8]. This episodic phenomenon has been associated with precipitation anomalies across China [9–11], especially over low-latitude

regions [12]. For example, Zhou and Wu [13] revealed that the deflection of lower-level southwesterly winds from the southeast coast of China, as well as the subsequent effect on winter precipitation in southern China, could be primarily attributed to warm ENSO events. Specifically, significant and abundant precipitation was observed over both southern China and eastern central China in the autumn of an El Niño-developing year, coupled with an anomalous anticyclone over the western North Pacific. Given the strength differences and irregular phase changes within each ENSO cycle [14], ENSO-driven environmental events are extremely complicated, and their accurate prediction is very challenging. Thus, in recent decades, there has been a widespread increase in public concern regarding such events. Among the dangers associated with ENSO events, the most severe are generally considered to be those related to climatological and hydrological processes [8].

On the other hand, the IOD is a more recently identified type of climate driver [15]. As an important mode of inter-annual variability in the tropical Indian Ocean [16], the IOD has been proposed as another significant factor influencing water circulation and rainfall in China [17–19]. In summer, owing to changes in the intensity of the South Asian High and the western North Pacific anticyclone, different phases of the IOD remotely influence monsoon-induced rainfall over China [19]. Furthermore, after examining the effect of IOD events on China's rainfall patterns during the boreal summer and autumn seasons, Qiu et al. [20] revealed the existence of asymmetric impacts of positive and negative IOD events in terms of their extratropical response. Additionally, IOD events influence winter precipitation variability in China via a wave train induced by heating anomalies that emanate from the Indo-western Pacific [21].

In previous studies, ENSO and IOD events have been compared, and their combined impact has also been investigated. For example, a study conducted by Xiao et al. [22] revealed that both ENSO and IOD events affect summer and autumn precipitation in the Yangtze River Basin (YRB), as well as winter precipitation along with the North Atlantic Oscillation (NAO). Moreover, Xiao et al. [23] reported different regional responses to extreme precipitation in different phases of ENSO and IOD events. Further, based on a comparison of the impacts of ENSO, IOD, and NAO events, using data corresponding to the 1960–2014 period, Gao et al. [24] concluded that ENSO and IOD events have more severe effects on the intensity, frequency, and duration of extreme precipitation than NAO events. Furthermore, based on observations during simultaneous ENSO and IOD events, Weng et al. [19] suggested that the effects of one phenomenon on the summer climate in different regions of China may be enhanced or weakened by those of the other. Xu et al. [25] studied the possible impacts of ENSO and IOD events on boreal autumn rainfall anomalies in China and reported that the positive phase of the combination of ENSO and IOD events can increase autumn rainfall over southern China owing to the development of an anomalous lower-level anticyclone over the western North Pacific region. Pillai, P.A. [26] recently published a paper analyzing the influence of the ENSO-IOD relationship on the major modes of Asian summer rainfall.

Most previous studies have explored the individual impacts of ENSO and IOD events on precipitation in China or the YRB [21,27,28]. However, their combined impact on regional streamflow in the JRB has rarely been investigated. Moreover, most previous studies have focused only on the impact of ENSO events on streamflow [8]. Therefore, it is necessary to analyze the impacts of both ENSO and IOD events on the temporal and spatial patterns of regional streamflow in the JRB. Reportedly, extreme precipitation events also play an important role in flood control and ecology protection [29,30], implying that the effects of ENSO and IOD events on extreme precipitation conditions should also be investigated. Additionally, some studies analyzed the impacts of ENSO and IOD events throughout the period of their occurrence [4,31]; however, the results were unclear because the lag effect of the climate anomalies was not fully considered [27]. Therefore, to avoid missing any information on the impact of these climate anomalies, both their developing and decaying years were considered in this study.

The objective of this study is to explore the impacts of ENSO and IOD events on streamflow in the JRB. Based on continuous data series collected at a control hydrological station in the JRB (Xiangjiaba Station) during 1961–2016, the wavelet coherence method is introduced to analyze the correlation between streamflow anomalies and the two climate drivers. To establish several scenarios, the study period is divided into several shorter periods, including neutral years, pure ENSO (El Niño/La Niña) years, IOD (positive/negative) years, and combined ENSO and IOD years based on an analysis of monthly series data of Niño 3.4 indices and the Dipole Mode Index (DMI). Annual and seasonal streamflow data, as well as their temporal and spatial distributions under the different scenarios, are compared with those of the neutral scenario. Additionally, the impact of the climate drivers on extreme precipitation conditions is also analyzed, which is presented as the 1-day/3-day/7-day stream flow maxima/minima. To reveal and clarify the connection between the climate drivers and streamflow, the impacts of ENSO and IOD events on precipitation are analyzed. Finally, to facilitate the sustainable use of water resources and ensure the effective control of disasters such as floods, recommendations for water resource management are proposed based on the impacts of ENSO/IOD events on streamflow characteristics. The results of this study will advance our understanding of hydrological processes in the JRB and have important applications for flood and drought disaster prevention, water resource planning, hydropower generation, and agriculture in the JRB.

2. Materials and Methods

2.1. Study Area

The JRB is located between 24°36′–35°44′ N latitude and 90°30′–105°15′ E longitude in southwestern China. The JRB is at the head of the Yangtze River basin, covering an area of 473,200 km^2 with an elevation difference of up to 5142 m [32]. The mainstream of the JRB has a length of 3486 km and flows from the Qinghai-Tibet Plateau to Yunnan and Sichuan provinces. The largest tributary, called Yalong River, merges with the mainstream at Panzhihua City, Sichuan Province [33]. There are four hydrological stations in the JRB, including Zhimenda, Shigu, Tongzilin, and Xingjiaba stations. Based on the distribution of these stations, as well as the digital elevation model, the JRB can be divided into four sub-basins: the source region of the JRB (SRJRB), the upper part of the JRB (UPJRB), Yalong River basin (YLRB), and the middle and lower part of the JRB (MLJRB). The location of hydrological and meteorological stations and the distribution of the sub-basins are shown in Figure 1.
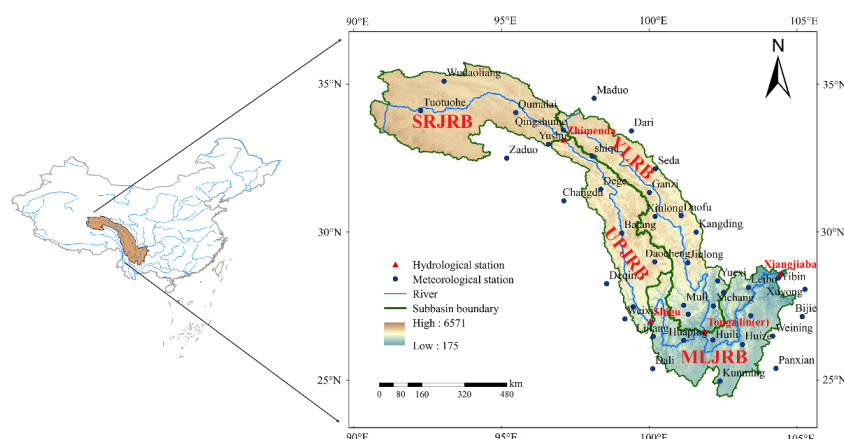

Figure 1. Location of hydrological and meteorological stations, the digital elevation model, and sub-basin boundaries in the Jinsha River Basin, China. The sub-basin boundaries are based on the distribution of hydrological stations and the digital elevation model. Zhimenda, Shigu, and Xingjiaba Stations are located on the main channel while Tongzilin is located on the tributaries. Zhimenda, Tongzilin, and Xiangjiaba are the hydrological control stations of the Source region of the Jinsha River Basin (SRJRB), Yalong River Basin, and the whole Jinsha River Basin.

The JRB is important not only for regional economic development and environmental protection, but also for national hydropower generation, flood control, and water resource allocation. The total exploitable installed capacity of the JRB for power generation is 59,080 MW, which is approximately one-sixth of that of China. Thus, the JRB plays an important role in China's "West to East Power Transmission Project" and contains four large hydropower stations in the downstream area, including Wudongde and Baihetan (under construction) and Xiluodu and Xiangjiaba (in operation), the capacity of which is more than double that of the Three Gorges hydropower station [3]. Moreover, reservoir operation in the JRB not only protects important cities and towns such as Chongqing and Yibin from floods but also prevents floods in the middle and lower reaches of the Yangtze River via cooperating with the Three Gorges Dam [2]. Furthermore, according to the South-to-North Water Transfer Project plan, the JRB is the main source of the West Route of the South-to-North Water Transfer project, which aims to transfer 17 billion m3/year of water to the north-western provinces [34].

2.2. Data

The datasets used in this study are as follows: (1) Monthly average streamflow data of the four hydrological stations in the JRB that have continuous data series from 1961–2016. (2) Daily streamflow data from the four hydrological stations of the JRB that have continuous data series from 1964–1986 and 2007–2016. (3) Monthly mean precipitation at 40 meteorological stations in or around the JRB for the period of 1961–2016, obtained from the China Meteorological Administration (http://data.cma.cn/ accessed on 6 November 2021)). Annual and seasonal air temperature data and precipitation data in the JRB and its four sub-basins were derived from Mendeley data: 10.17632/5hpn8jcrbt.1. (4) Monthly sea surface temperature anomaly data in the Niño 3.4 region for the period of 1950–2016 collected from NOAA (http://www.cpc.ncep.noaa.gov/products/analysis_monitoring/ ensostuff/ensoyears.shtml accessed on 10 December 2021)). (5) The Dipole Mode Index (DMI) from 1870 to the present, maintained by the Japan Agency for Marine-Earth Science and Technology (http://www.jamstec.go.jp/frsgc/research/d1/iod/iod/dipole_mode_ index.html (accessed on 10 December 2021)) [22]. The application diagram of all of the data is shown in Figure 2.
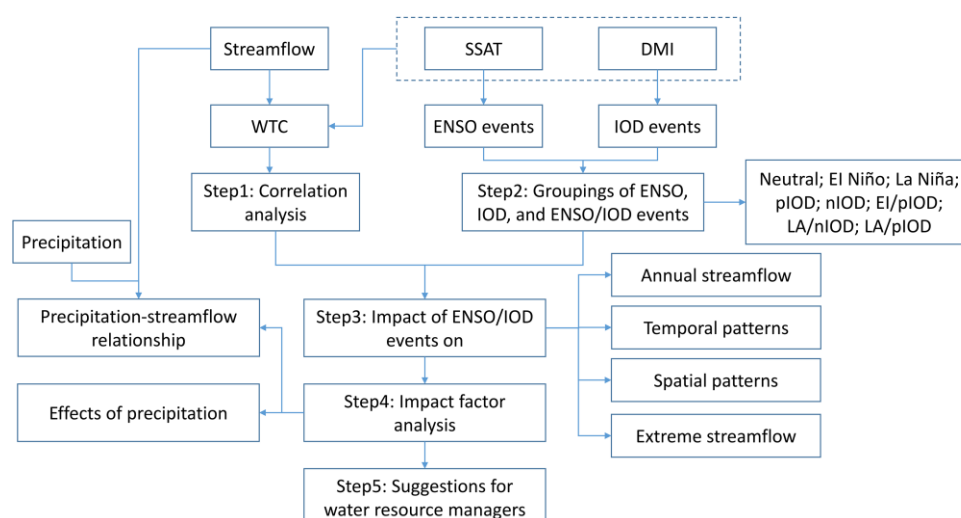

Figure 2. Application of the data.

Data uncertainty mainly includes observation of data quality and interference caused by human activities. In this study, the data used in this paper were collected from the "Changjiang Water Resources commission of the Ministry of Water Resources", the manager of the Jinsha River Basin, which has been validated and widely used in previous studies. Moreover, we doubled check the data quality by using the RClimDex software (http:

//etccdi.pacificclimate.org/software.shtml (accessed on 12 December 2021)). To be specific, any identified potential outliers (such as typing errors, missing data, and rejected values) were manually checked and corrected.

Additionally, several large reservoirs have been built in the Jinsha River basin in recent years. To exclude the impact of human activities in this study, we put the series before and after the reservoir construction together for grouping. The main advantages of this grouping are (1) the disturbing of human activities in the study conclusion could be ignored according to the difference between groups, and (2) we could make full use of the latest sample data as much as possible.

2.3. Wavelet Coherence and Correlation Analysis

Wavelet transforms coherence (WTC) methods, which can be used to quantify the coherence of cross-wavelet transform in a time–frequency space, have been widely used to analyze geophysical process [8,34,35]. The advantage of this method is that, even if the common power is low, WTC can identify significant coherence signals because it provides localized correlation for each frequency and time scale. The coherence was defined by the following equation [15]:

$$R_n^2(s) = \frac{\left| Ss^{-1} W_n^{XY}(s) \right|^2}{Ss^{-1} |W_n^X(s)|^2 Ss^{-1} |W_n^Y(s)|^2} \tag{1}$$

where $R_n^2(s) \in [0, 1]$ and can be conceptualized as a localized correlation coefficient in time and frequency space [36]. See Zhang et al. [34] for more details regarding WTC.

In this study, WTC was used to analyze the relationship between annual monthly sea surface temperature anomaly and annual streamflow anomalies, as well as that between the DMI from August through November and annual streamflow anomalies [37] in the JRB. Furthermore, in order to consider different phases of ENSO and IOD events and the lag effect of their impact on streamflow [8,27], the correlations in developing years (Table 1) and decaying years (one year later) were also analyzed.

Table 1. Groupings of ENSO, IOD, and ENSO/IOD events during 1961–2016. The number of years corresponding to each grouping is shown in parentheses at the end of each grouping.

|	**Positive IOD (pIOD)**	**Neutral**	**Negative IOD (nIOD)**
El Niño	1963, 1972, 1982, 1991, 1994, 1997, 2006, 2015 (8)	1965, 1969, 1977, 1983, 1987, 2002, 2009 (7)	Nil (0)
Neutral	1961, 2003, 2007, 2012 (4)	1962, 1966, 1967, 1968, 1976, 1978, 1979, 1980, 1981, 1985, 1986, 1990, 1993, 1995, 2004, 2005, 2014 (17)	1984, 1992, 1989, 1996, 2001, 2013 (6)
La Niña	1970, 2008, 2011 (3)	1971, 1973, 1975, 1988, 1999, 2000 (6)	1964, 1974, 1998, 2010, 2016 (5)

2.4. Classification of ENSO and IOD Years

There is no single internationally sanctioned definition of ENSO and IOD events as they differ according to different research purposes or organizations [4]. This study adopts the definition of ENSO employed by NOAA, that is, "a warm (cold) ENSO event that occurs if the three-month running means of sea temperature (SST) anomalies in the Niño 3.4 region (5° N–5° S, 120°–170° W) exceed + (−)0.5 °C for five months or more" (Wei et al. 2019). IOD events were determined based on monthly values of the DMI (Saji et al. 1999), which represent the SST anomaly difference between the western equatorial Indian Ocean (50°–70° E, 10°S–10° N) and the southeastern equatorial Indian Ocean (90°–110° E, 10° S–0° N). IOD events are deemed to occur if the monthly DMI value exceeds 0.75 of the standard deviation in this study, which is similar to that of a previous study (Jarvis et al. 2018). A pure ENSO (or IOD) event was identified when it was not accompanied simultaneously by IOD (or ENSO), while a combined event was defined as ENSO and IOD

peaking at the same time [38,39]. A Diagram of scenarios for the whole series is shown in Figure 3a, which means that if the orange line is higher than the red dotted line above and lasts for more than 5 months, the EI Nino event occurs.
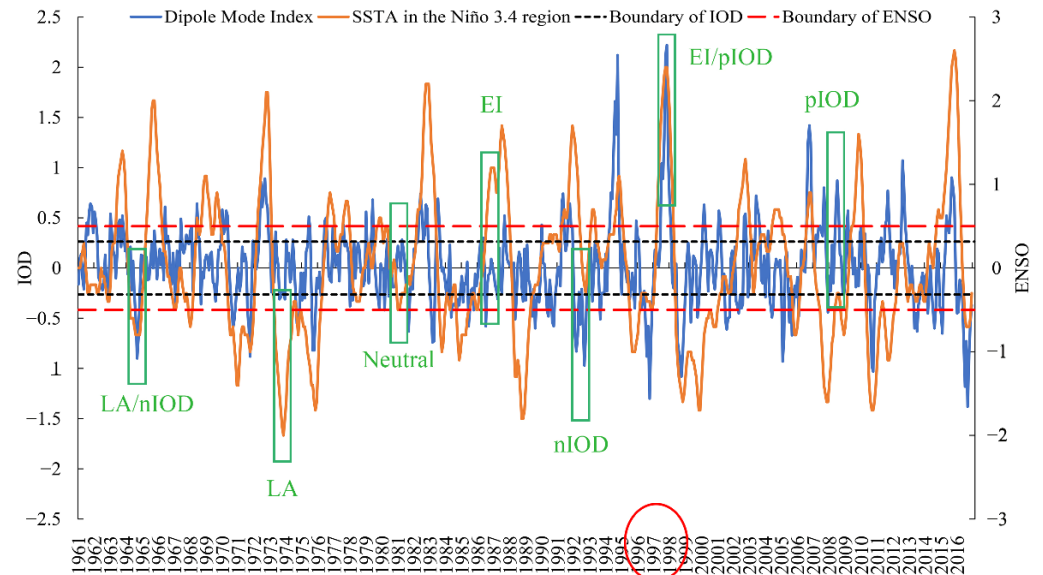
(a)
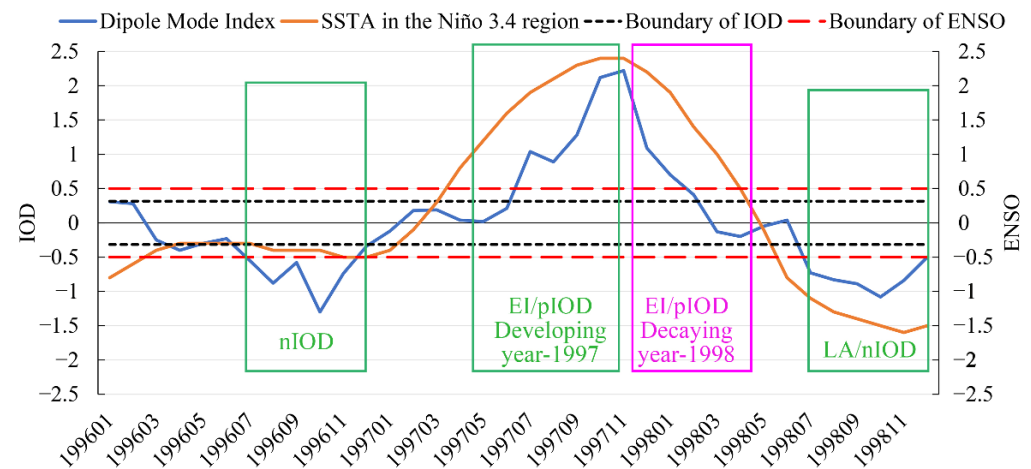
(b)

Figure 3. (**a**) Diagram of scenarios for the whole series; (**b**) Diagram of scenarios of the typical period from 1996 to 1998, which is highlight by the red circle in (**a**).

In this study, the developing year is treated as the year when climatic anomaly indices reach a peak value, with the decaying year identified as the following year, which was shown in Figure 3b. Following the aforementioned criteria, ENSO and IOD developing year classifications are shown in Table 1. These classifications are in good agreement with other studies and capture the major events [40]. Furthermore, spring is defined as March to May, summer is from June to August, autumn is from September to November, and winter is from December to February of the following year.

3. Results

3.1. Correlation between ENSO/IOD Events and Streamflow Anomalies

Xingjiaba Station was the control hydrological station for the JRB (Figure 1). Based on annual continuous data series collected at this station, the WTC method was introduced to analyze the correlation between ENSO/IOD events and streamflow anomalies, which is shown in Figure 4 [36].
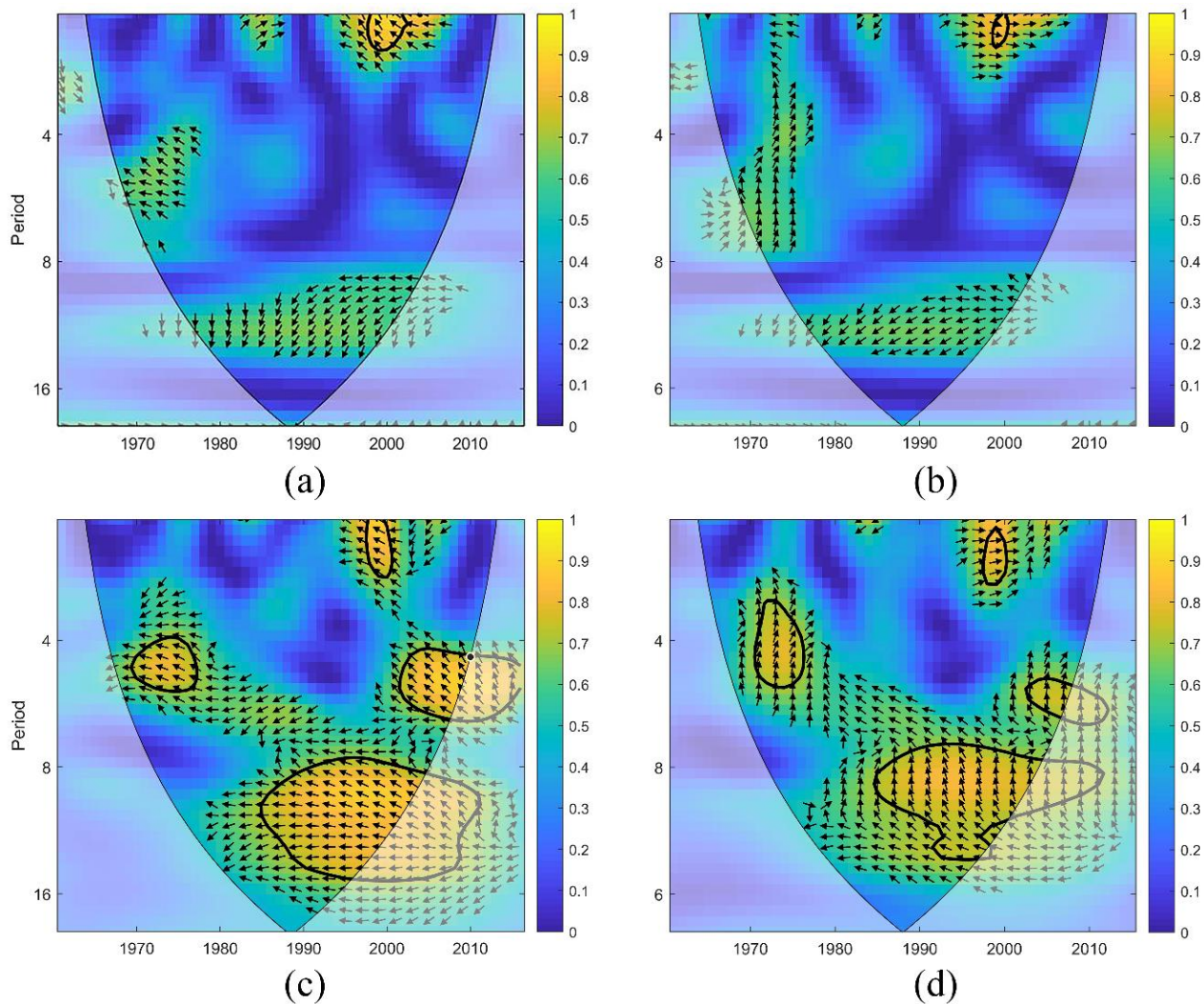

Figure 4. Differences between the streamflow anomalies and ENSO indices (first row) as well as IOD indices (second row) were obtained using the WTC method. (**a**,**c**) Developing years, (**b**,**d**) Decaying years. Areas enclosed by thick lines represent statistically significant coherence at a 5% significance level concerning noise (yellow) based on the Monte Carlo simulation method. Arrows indicate wavelet coherences above 0.5, which represent the phase difference of the oscillations. The arrows pointing right show in-phase coherence, whereas those pointing left show anti-phase coherence.

Figure 4a,b show the 1-year cycles of the isolated coherence between streamflow anomalies and ENSO events, which were primarily anti-phase. The statistically significant wavelet coherences predominantly corresponded to the 1998–2004 period, and the coherences were greater than 0.5 during the 1970s and within the 1983–1986 period. The index of the Niño 3.4 was greater than two during all these periods, indicating a significant correlation between strong ENSO events and streamflow anomalies in the JRB. Comparing Figure 4a,b reveals an opposite shift in the phase difference when the period was

less than eight years, i.e., the coherence changed from in-phase to anti-phase during the 1998–2004 period.

Figure 4c,d show a more significant correlation between IOD events and streamflow anomalies. Zhang et al. [34] noted that the upper Yangtze River is influenced by the Indian summer monsoon, which could be partly responsible for the different correlations between IOD and ENSO. Throughout the study period, scattered coherences (primarily anti-phase) between streamflow anomalies and IOD events were detected that predominantly corresponded to 1–15-year cycles. Additionally, 4–6-year statistically significant wavelet coherences were primarily detected within the 1970–1975 period and after 2000, whereas 1–2-year and 8–15-year statistically significant wavelet coherences were primarily detected within the 1998–2000 and 1985–2010 periods, respectively. The phase difference shifted from ∼135° in developing years to 45° in decaying years for the 1998–2000 period, whereas no apparent phase changes were observed within other periods.

3.2. Impact of ENSO/IOD Events on Annual and Seasonal Streamflow

The impact of ENSO/IOD events on annual and seasonal streamflow anomalies is shown in Figure 5, which revealed that ENSO and IOD events had different impacts on streamflow anomalies in different phases.
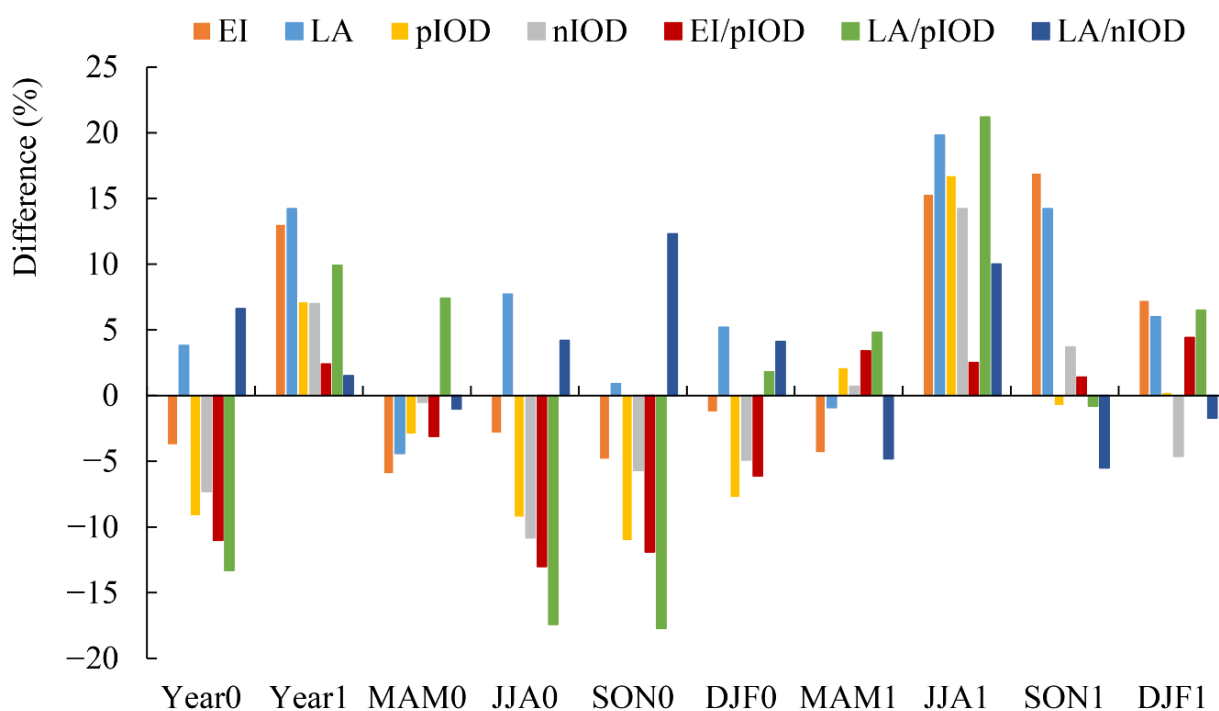

Figure 5. The relative difference of annual and seasonal streamflow in different groups of ENSO and IOD events in the Jinsha River Basin (1961–2016). (0, developing year; 1, decaying year; MAM, March-April-May; JJA, June-July-August; SON, September-October-November; DJF, December-January-February. Note: Difference = (streamflow in ENSO/IOD years − streamflow in neutral years)/streamflow in neutral years * 100).

In developing years, except for La Niña events and their simultaneous occurrence with negative IOD (nIOD) events, fewer annual streamflow anomalies were observed relative to neutral years. Even though all differences were below 10%, the impact of pure IOD events was twice that of pure ENSO events. Additionally, when La Niña and nIOD events occurred simultaneously, the streamflow anomaly was twice as severe as that corresponding to the occurrence of pure La Niña events.

In decaying years, the annual streamflow anomaly in the JRB was more severe than that observed in neutral years, regardless of the type of streamflow anomaly observed, and

the impact ranged from 1.5–14.2%. The streamflow corresponding to the occurrence of pure ENSO events (∼14%) was twice that corresponding to the occurrence of pure IOD events (∼7%). Additionally, the simultaneous occurrence of EI Niño and pIOD (or La Niña and nIOD) events had a less severe impact (<3%) than pure ENSO or IOD events. Although the simultaneous occurrence of La Niña and pIOD events resulted in 10% more streamflow relative to neutral years, it was obvious that the difference was smaller than that resulting from the occurrence of pure La Niña events (14%).

Seasonal analysis showed that the impact of the climate indices on streamflow in summer and autumn were primarily responsible for the annual streamflow observed in the JRB. Notably, all streamflow amounts that were more than 10% larger than neutral year streamflow were observed in summer and autumn in both developing and decaying years, i.e., ∼80% of the total amount of streamflow observed within a year was attributed to streamflow in summer and autumn. Specifically, the impact of ENSO events on streamflow was more severe in the summer and autumn of decaying years, whereas that of IOD events was more severe in the autumn of developing years and the summer of both phases. Although the impact of the simultaneous occurrence of ENSO and IOD events was more complex, compared with pure ENSO or IOD events, it resulted in higher differences in June-July-August-0 (JJA0), September-October-November-0 (SON0), and JJA1 for most cases, especially for the simultaneous occurrence of La Niña and pIOD events.
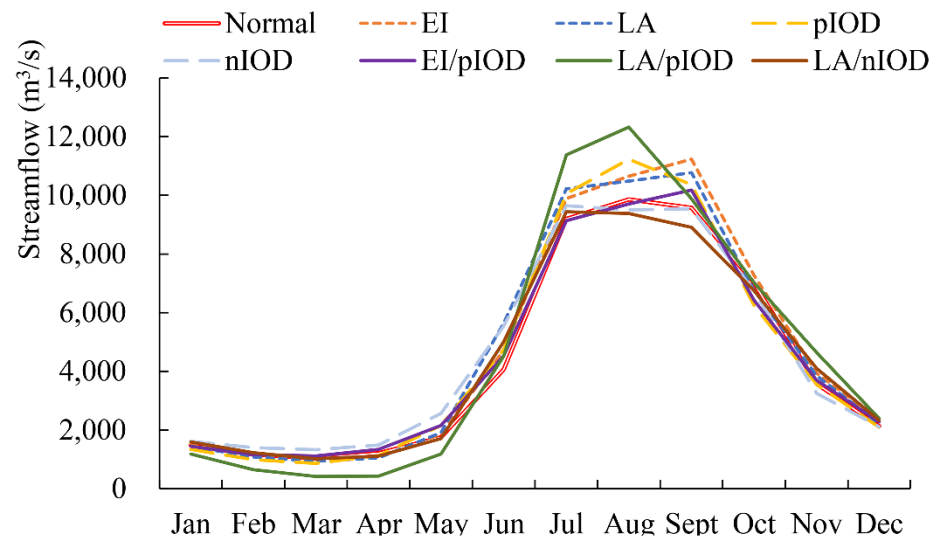
3.3. Temporal Patterns of Climate Driver Impacts

The differences between monthly streamflow amount corresponding to the different cases are shown in Figure 6, with Figure 6a showing the streamflow distribution for different groups of events. In developing years, the streamflow corresponding to neutral years (red line) showed a single-peak-shaped trend, which tended to increase from March to September, before decreasing until March the following year, with a peak streamflow value of 10,551 m^3/s. When pure ENSO events occurred, the peak value of streamflow shifted from September to August, i.e., one month earlier relative to neutral years. Regarding the occurrence of pure EI Niño events (brown dotted line), the peak streamflow observed in August was 10% less than that in neutral years. However, for pure La Niña events (blue dotted line), the peak streamflow observed in August was 10% higher than that in neutral years. Additionally, when pure IOD events occurred, the streamflow peak seemed to drop from 10,551 to 9000 m^3/s, then remained stable from July to September, and the simultaneous occurrence of ENSO and pIOD events resulted in a monthly streamflow pattern that was similar to that corresponding to pure pIOD events. However, the distribution of streamflow corresponding to the simultaneous occurrence of pure La Niña and pure nIOD events was very similar to that of pure La Niña events. Moreover, in September, the peak streamflow value of this combination reached 12,260 m^3/s, which was 15% higher than the peak value in neutral years.

The streamflow distributions in decaying years are shown in Figure 6b. In the neutral year (red line), the streamflow in the JRB also showed a single-peak-shaped trend. Additionally, the streamflow distributions corresponding to pure EI Niño and La Niña events were similar. When pure ENSO events occurred within the July–October period, streamflow was higher than that in neutral years, especially when the streamflow peaked in September, representing a 25% increase relative to neutral years. However, when pIOD events occurred, the peak streamflow observed in August was three times greater than that corresponding to nIOD events. Regarding the simultaneous occurrence of EI Niño and pIOD events, as well as La Niña and nIOD events, the streamflow distributions were close to those of neutral years. However, the simultaneous occurrence of La Niña and pIOD events produced the peak streamflow value one month earlier than neutral years, as well as the highest streamflow in July and August, which was 25% and 36% higher than that in neutral years, respectively.
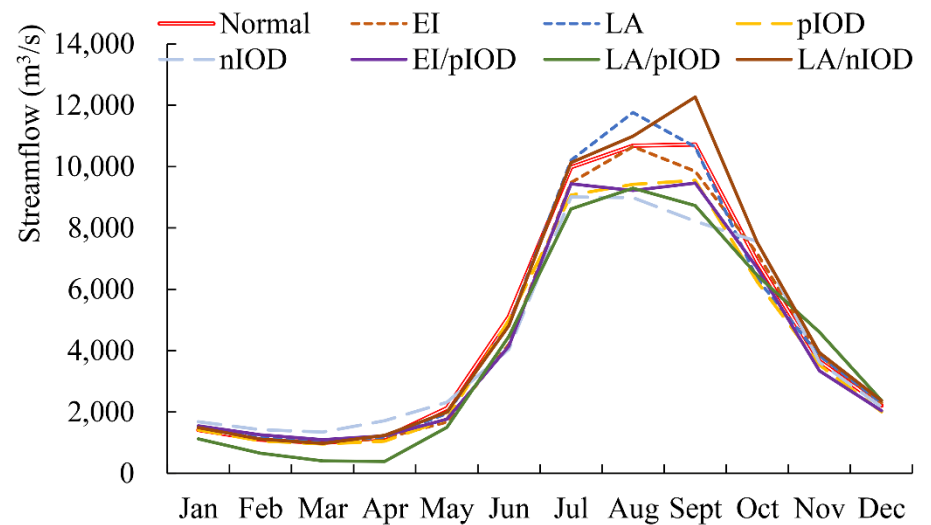
Figure 6. Streamflow distribution in neutral years and those corresponding to ENSO/IOD event years in (**a**) developing years and (**b**) decaying years.

3.4. Spatial Patterns of Climate Driver Impacts

The JRB was divided into four different sub-basins according to the location of hydrological stations, and the digital elevation model was used to analyze the spatial patterns of the impact of climate indices on streamflow. Four different sub-basins were designated, including SRJRB, UPJRB, YLRB, and MLJRB, each of which contained control hydrological stations, i.e., Zhimenda, Shigu, Tongzilin, and Xiangjiaba stations, respectively. The streamflow corresponding to each sub-basin was calculated based on the data collected at each hydrological station, and their proportions in the JRB are shown in Figure 7a. The YLRB sub-basin was the greatest contributor to streamflow in the JRB (~41%), followed by MLJRB (~30%), and UPJRB (20%), with the lowest contribution from the SRJRB substation (~9%).
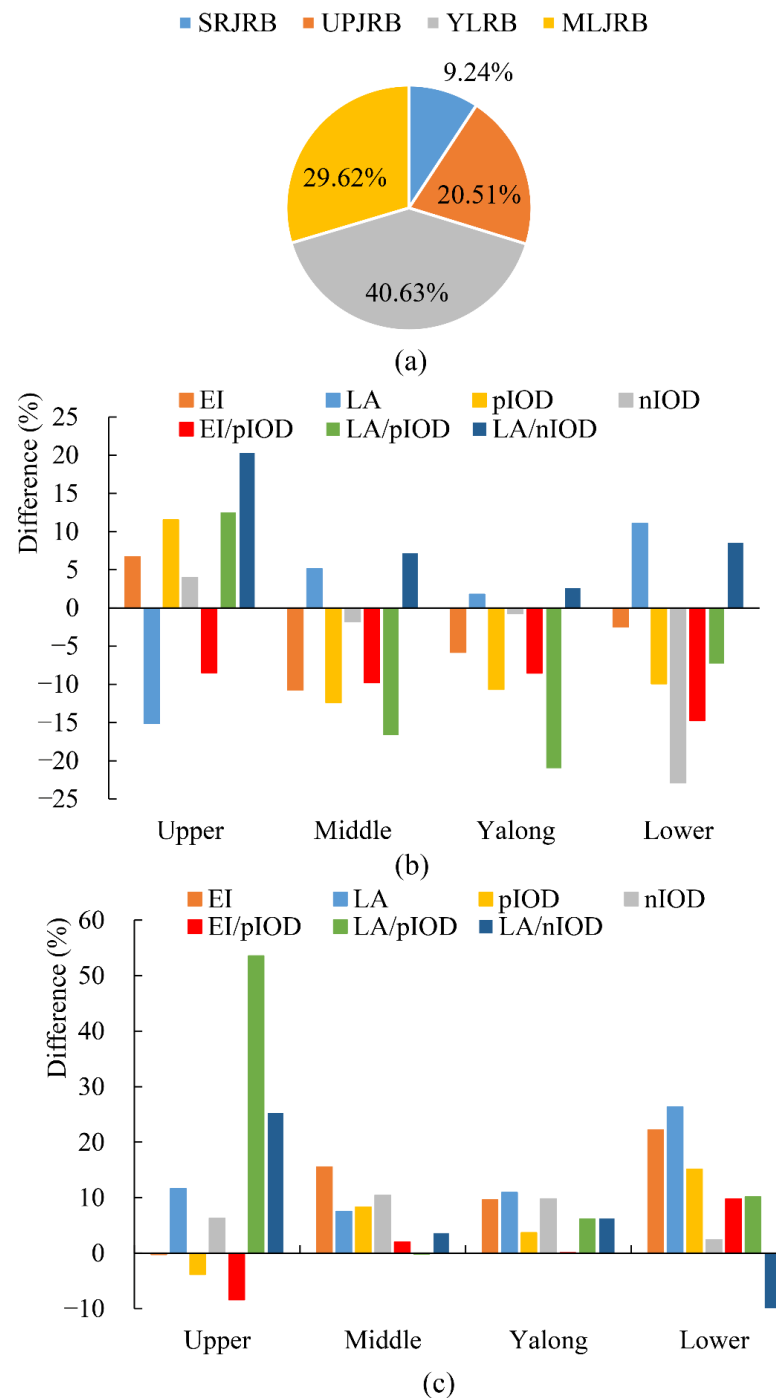
Figure 7. (**a**) Streamflow proportions of the four sub-basins in the Jinsha River Basin. Annual streamflow in different sub-basins relative to those corresponding to neutral years in, (**b**) developing years, and (**c**) decaying years.

The annual spatial distribution of streamflow in developing years is shown in Figure 5b for the different sub-basins. Generally, the impact corresponding to the MLJRB and YLRB were quite similar in all cases. The MLJRB also showed a similar impact, with only slight differences, whereas the SRJRB showed the opposite impact in most cases. Specifically, during pure El Niño events, which showed the most severe impact of all climate indices, streamflow in the UPJRB was 10% less than that in neutral years. For pure La Niña events in the developing years, streamflow in the SRJRB was only 85% of that in neutral years. However, streamflow in the MLJRB was 10% higher relative to neutral years. Regarding

pIOD events, streamflow was 10% higher than that in neutral years in the SRJRB but 10% lower in all other sub-basins. Additionally, 20% more streamflow was observed in the MLJRB during nIOD events; however, the impact on streamflow in the other sub-basins was less than 5%. When EI Niño and pIOD events occurred simultaneously, the streamflow in all sub-basins was lower than that in neutral years by 8% (SRJRB) to 15% (MLJRB), whereas the simultaneous occurrence of La Niña and nIOD events resulted in more streamflow, which was 3% (YLRB) to 20% (SPJRB) higher than that in neutral years. Additionally, the simultaneous occurrence of La Niña and pIOD events resulted in 15% less streamflow in the YLRB and MLJRB, but 10% more streamflow in the SRJRB relative to neutral years. This could be related to the fact that the elevation of SRJRB is significantly higher than in other regions. However, the impact of ENSO and IOD on runoff at different elevations needs further study.

Figure 7c shows the spatial distribution of streamflow amounts in decaying years. In most cases, streamflow was higher than that in neutral years for all sub-basins. Additionally, the simultaneous occurrence of ENSO and IOD events had a greater impact on streamflow in the SRJRB, whereas pure ENSO events had a greater impact on streamflow in the MLJRB. Specifically, in decaying years, pure ENSO events had the most significant impact on streamflow in the MLJRB (20% greater than that in neutral years). Except for the MLJRB, owing to the occurrence of pIOD events, the impact of pure IOD events on streamflow was less than 10% in the three other sub-basins. There was no apparent difference in streamflow resulting from the simultaneous occurrence of EI Niño and pIOD events in any sub-basin (<10% that of neutral years). However, when La Niña and pIOD events occurred simultaneously, streamflow in the MLJRB increased by half, whereas that in the other sub-basins exhibited a smaller increase (below 10%).

3.5. Impact of ENSO/IOD Events on Annual Extreme Streamflow Conditions

Extreme precipitation conditions, including the annual maxima and minima 1-day/3-day/7-day mean flows, play a key role in the occurrence of floods and droughts, and have substantial potential applications in water resource management. Loss of lives and infrastructure, as well as the economic disruption caused by flooding, may result from extreme annual precipitation. Additionally, both the direct and indirect effects of floods can last for decades [41].

Figure 8 shows the different streamflow1-day/3-day/7-day maxima resulting from the climatic indices in the developing years relative to those in neutral years. The results corresponding to the three indices (1-day/3-day/7-day) were consistent, i.e., the impact of climate indices on the streamflow maxima led to clearly higher streamflow than the annual or seasonal average streamflow. The highest streamflow maxima, which was observed at Zhimenda Station during the simultaneous occurrence of La Niña and pIOD events, was 50% more than that in neutral years. Different phases of ENSO and IOD events also showed different impacts on the streamflow maxima. Specifically, the impact of pure IOD events in developing years was higher than that of pure ENSO events, implying that more attention should be paid to the simultaneous occurrence of La Niña and nIOD events in the developing year owing to the increased streamflow maxima (~10%) observed at all stations. This increase is consistent with the results of the annual and seasonal streamflow analysis.

In the decaying years (Figure 9), when pIOD events occurred or when EI Niño and pIOD events occurred simultaneously, the impacts on streamflow at the four sub-basins were less than 10% of those in neutral years. However, positive impacts were dominant in the other cases. Pure ENSO events appeared to result in 20% more streamflow at Shigu and Xiangjiaba Stations. However, much more attention should be paid to the occurrence of nIOD events as well as the simultaneous occurrence of La Niña and nIOD events given that the streamflow maxima corresponding to these years were higher at all stations than those in neutral years (>10–50%).
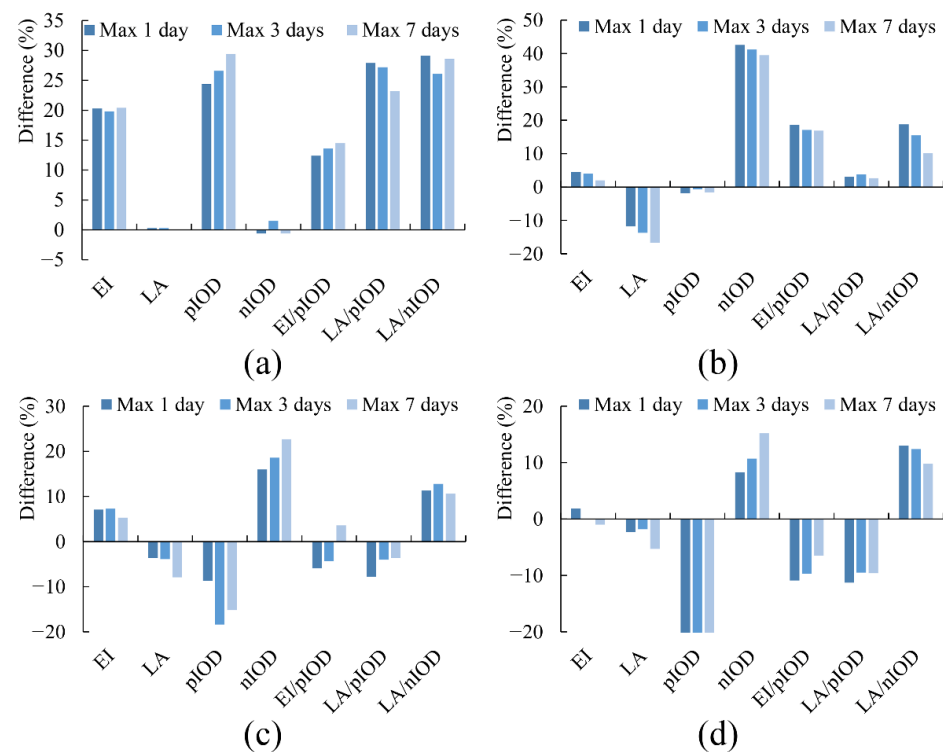
Figure 8. The difference in 1-day/3-day/7-day maxima streamflow relative to neutral years in developing years at (**a**) Zhimenda, (**b**) Shigu, (**c**) Tongzilin, and (**d**) Xiangjiaba. Note: Difference = (maximum streamflow in ENSO/IOD years—maximum streamflow in neutral years)/maximum streamflow in neutral years * 100.
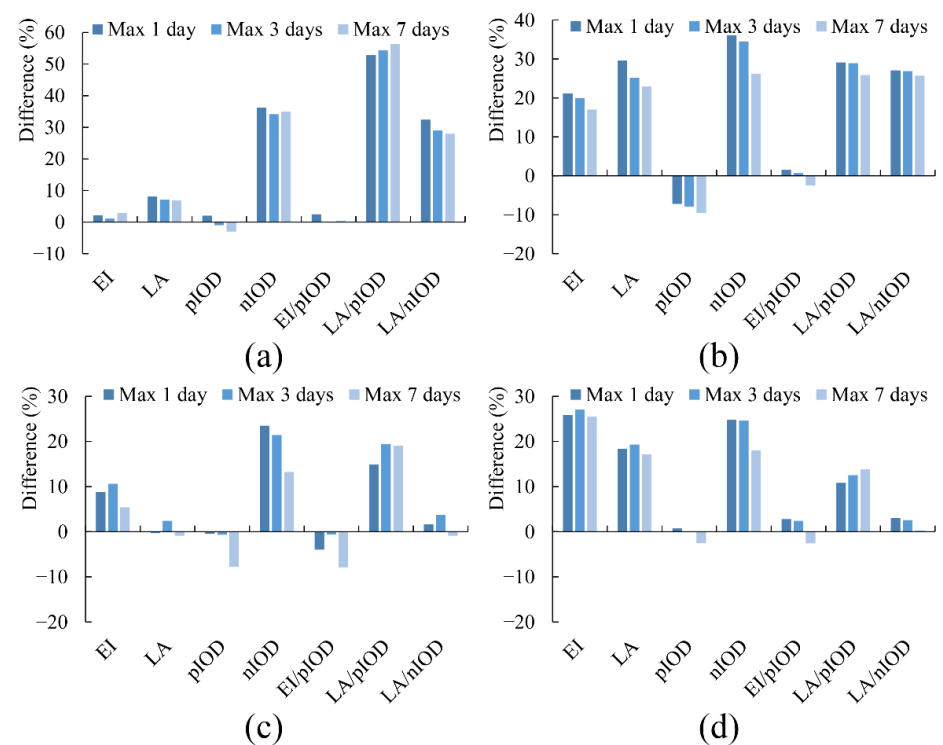

Figure 9. The difference in 1-day/3-day/7-day maxima streamflow relative to neutral years in decaying years at (**a**) Zhimenda, (**b**) Shigu, (**c**) Tongzilin, and (**d**) Xiangjiaba.

Figures 10 and 11 show the impact of climate indices on the streamflow minima corresponding to 1-day/3-day/7-day streamflow. Unlike the streamflow maxima, the streamflow minima corresponding to the three indicators were different in most cases. The streamflow minima at Zhimenda Station was the lowest; therefore, attention should be paid to the occurrence of nIOD events in the developing year considering that they result in 30% less streamflow at this station. At the other stations, in both developing and decaying years, the impact in most cases was less than 10%.
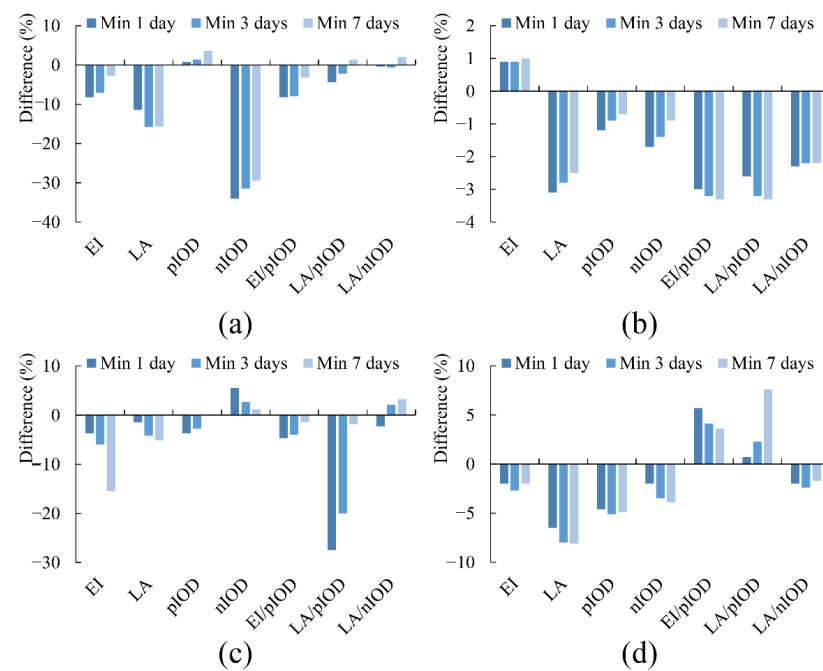

Figure 10. The difference in 1-day/3-day/7-day minimum streamflow relative to neutral years in developing years at (**a**) Zhimenda, (**b**) Shigu, (**c**) Tongzilin, and (**d**) Xiangjiaba.
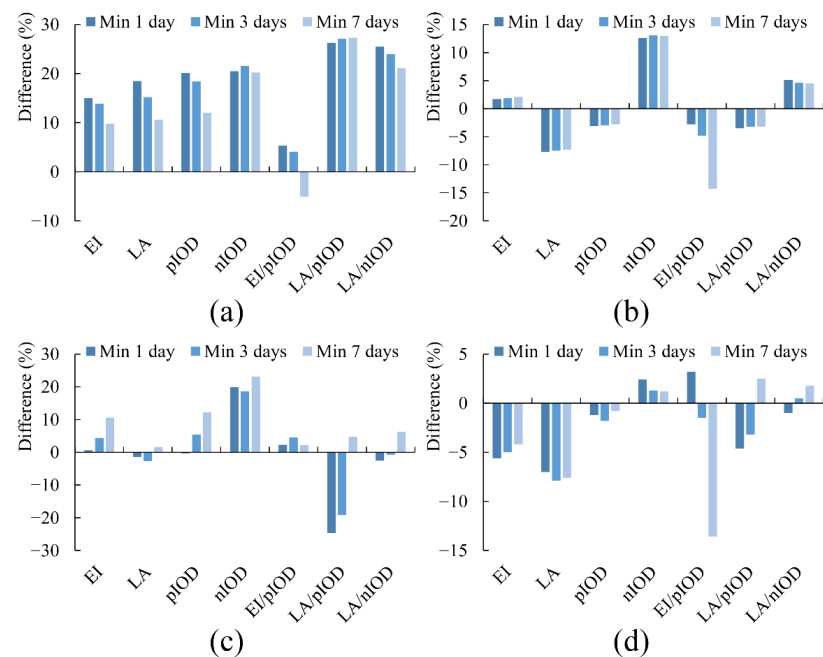

Figure 11. The difference in 1-day/3-day/7-day minimum streamflow in decaying years in developing years at (**a**) Zhimenda, (**b**) Shigu, (**c**) Tongzilin, and (**d**) Xiangjiaba.

4. Discussion

4.1. Precipitation-Streamflow Relationship

Precipitation is considered one of the main driving factors of streamflow or streamflow variations; the precipitation-streamflow relationship is not only important for water resource management, but it also plays an important role in watershed system evolution [42]. Based on the results of the Pearson correlation test, the correlation coefficient of the relationship between streamflow and precipitation in the JRB was 0.7, whereas that in the SRJRB, UPJRB, MLJRB, and YLRB sub-basins was 0.71, 0.62, 0.51, and 0.83, respectively. At a 95% confidence interval, all correlation coefficients were significant.

As shown in Figure 10a,b, and compared with Figure 5, the climate indices had a somewhat similar impact on precipitation and streamflow. The percentage change in streamflow as a function of the percentage change in precipitation and temperature is shown in Figure 10c, which reveals an approximately equivalent variation in these parameters across the JRB, i.e., the percentage increase or decrease in streamflow was always greater than that of precipitation. A similar conclusion was reported for changes in the Sacramento Basin [43] and Yellow River Basin [4], although the magnitude of changes differs. Except for the small increase in precipitation (<+3%), the streamflow percentage change in the JRB was greater than the precipitation percentage change.

4.2. Effects of Precipitation

4.2.1. Pure ENSO Events

Figure 12a shows that, in developing years, the occurrence of EI Niño events resulted in less precipitation compared to neutral years, whereas the opposite phenomenon was true for the occurrence of La Niña events; this finding is consistent with the results obtained for streamflow and is also supported by previous studies. For example, based on the results of χ^2 tests, Tong et al. [44] reported a close relationship between El Niño and drought events, as well as a correlation between flood events observed in the upper Yangtze catchment during the 1868–2003 period and the occurrence of La Niña events. It has also been reported that EI Niño events could reduce precipitation in the source region [8]. Additionally, the results of a study on EI Niño months conducted by Ouyang et al. [45] showed a decrease in precipitation in most parts of the JRB owing to the occurrence of El Niño events. The mechanism of this impact was discussed by Li and Zhao [39], who explained that the transport of water vapor to eastern China during the developing spring is prevented by a Philippine Sea anticyclone (PSAC). Simultaneously, an anti-cyclonic moisture circulation anomaly appears in Mongolia, which also reduces the amount of precipitation observed over most parts of China, including the JRB.

As shown in Figure 12b, in the decaying years of pure ENSO events, the precipitation observed in the four sub-basins was greater than that in neutral years; thus, the annual streamflow in the JRB increased by 15% relative to neutral years. Feng et al. [11] suggested that the occurrence of El Niño events resulted in more precipitation in the south of the Yangtze River in decaying years; this wet signal lasted until the subsequent summer season. Additionally, a previous study focused on ENSO months reported significant increases in precipitation in the lower part of the JRB owing to La Niña events [45], which is also consistent with the results of this study. The mechanism by which pure ENSO events influence precipitation in decaying years was discussed by Wei et al. [8], who showed that negative vertical velocity anomalies at the source of the Yangtze River, as well as abundant water vapor on the southeast side of the YRB in decaying years, play a more important role during the following summer than vertical velocity variations.

4.2.2. Pure IOD Events

Regarding pure IOD events, Hong et al. [31] reported very similar rainfall anomaly patterns over Far East Asia owing to the occurrence of both positive and negative pure IOD events. Their result is consistent with the results of this study, but contrary to the

findings of a study conducted in Australia, which revealed that pIOD and nIOD events exhibit "impact asymmetry" on rainfall [46].
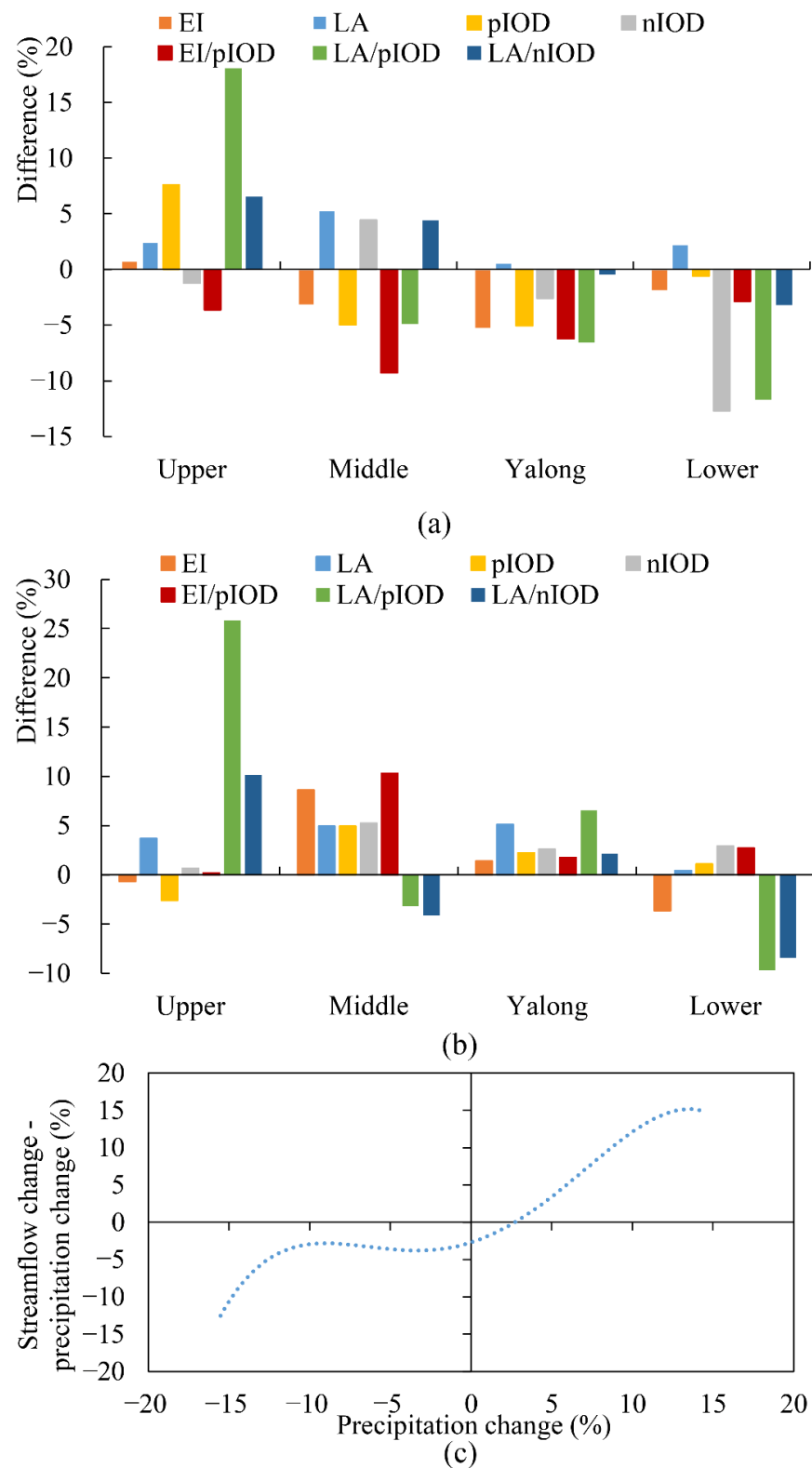

(a)

(b)

(c)

Figure 12. Annual precipitation in the different sub-basins and the entire Jinsha River Basin relative to neutral years in (**a**) developing years and (**b**) decaying years. (**c**) Percentage change in streamflow minus the percentage change in precipitation as a function of the percentage change in precipitation in the Jinsha River Basin.

In developing years, the occurrence of IOD events resulted in a 7% decrease in annual streamflow, whereas the observed precipitation was also lower than that in neutral years. Li and Zhao [39] attributed this observation to a cyclonic moisture circulation anomaly, whose center is located over the east side of Taiwan. This anomaly weakens the monsoonal northward wind originating from the oceans and results in a decrease in water vapor transport from tropical regions to the Yangtze River Valley. Regarding the decaying phase of pure pIOD events, Yuan et al. [47] elucidated that the high ridge of the 500-hPa western Pacific subtropical high advances westward to a greater extent, exerting control over southeast China, i.e., on the easterly anomalies on its south flank, thereby preventing water vapor transport from the Bay of Bengal into South China. Correspondingly, excessive rainfall occurs in Middle China, especially in the upper and middle reaches of the Yangtze River Valley; this explanation is also consistent with the results of this study.

4.2.3. Combination of ENSO and IOD Events

Climate-related studies investigating the impacts of ENSO and IOD events on seasonal variability have revealed that the most severe weather anomalies are observed when the two phenomena occur simultaneously [48]. This finding is also consistent with the results obtained in this study for developing years. According to Chang et al. [49], when El Niño and pIOD events occur simultaneously, anomalous cyclonic circulation shifts northwards toward Taiwan during the developing spring and summer. However, it is subsequently replaced by the PSAC in autumn, which is maintained until the following summer. Moreover, this cyclonic circulation is substantially intensified compared with observations corresponding to the occurrence of pure El Niño events. In decaying phases, southwesterly or southerly anomalies originating from the tropical oceans to North China, which are stronger than those corresponding to pure El Niño/pIOD events and accompanied by enhanced PSAC, were observed owing to the simultaneous occurrence of ENSO and IOD events.

4.2.4. Impact of ENSO and IOD Events on Extreme Precipitation

The impacts of ENSO and IOD events on extreme precipitation have also been investigated. Wan et al. [50] observed that the spatial regional patterns of extreme monthly precipitation, which showed greater variability in southern China than in northern China, were dependent on ENSO activities. Sun et al. [51] suggested that the 20–50% increase in extreme precipitation events observed once every 10 years in southeast China could be attributed to strong El Niño events and that the 10% increase in precipitation observed in northern Southeast Asia could be attributed to strong La Niña episodes. Additionally, Xiao et al. [23] reported different regional responses of annual extreme precipitation indices, including Max 1-day precipitation amount (Rx1day) and Max 5-day precipitation amount (Rx5day), to ENSO events at different stages, and that Rx1day is closely related to Rx5day, which is consistent with the results of this study. Furthermore, they noted generally positive correlations between these indices and ENSO events in the same year in the central part of China, whereas these positive correlations were observed one year ahead in the eastern part of China. Cheng et al. [52] also reported a particularly high correlation between dry/wet events and ENSO events in southwest China. Specifically, extremely dry/wet events occur during the ENSO period, whose frequency is approximately equal during El Niño and La Niña years.

Yuan et al. [47] observed excessive precipitation in the upper and middle parts of the YRB in the summer following pIOD events, which they attributed to the westward advancement of the 500-hPa subtropical high ridge and anomalous convergence of wind at 850 hPa over the middle part of the YRB during this period. Xiao et al. [23] also reported a positive correlation between extreme precipitation and 1-year ahead IOD events in central China. They also noted that IOD events at different stages result in different regional annual extreme precipitation response indices. Gao et al. [24] further reported that the effects of IOD events on extreme precipitation indices, such as RX1day, tended to become stronger

around the 1980s, and that IOD events might influence the convective available potential energy and play a role in flooding disasters over monsoon regions in China.

4.3. Suggestions for Water Resource Managers

The different streamflow characteristics resulting from the influence of different climatic indices in developing and decaying years compared with those in neutral years, as well as their potential impacts, are presented in Table 2, along with possible mitigation suggestions for water resource managers. In developing years, particular attention should be paid to potential droughts caused by the occurrence of pure IOD events and the simultaneous occurrence of ENSO and IOD events. On the other hand, the occurrence of pure ENSO events as well as the simultaneous occurrence of ENSO and IOD events in decaying years results in an increased risk of flood events, which can cause severe damage if countermeasures are not taken. However, the differences in streamflow amount corresponding to different temporal (annual/seasonal/7-day/3-day/1-day) and spatial (whole basin/sub-basin) scales present new challenges for water resource managers. Therefore, to eliminate fluctuations in water supply (i.e., the different precipitation conditions in each case) and demand (i.e., flood control, water supply, and hydropower generation), it is necessary to take advantage of relevant engineering measures, including reservoir operation and water transfer projects [53–55].

Table 2. Changes in streamflow characteristics and suggestions to water resource managers in each group.

	Developing Years		Decaying Years	
	Streamflow Characteristics Relative to Neutral Years	Suggestions	Streamflow Characteristics Relative to Neutral Years	Suggestion
EI	The peak streamflow value appeared one month earlier, and the streamflow in the middle JRB showed a decrease of more than 10%.	Reservoir managers should be cautious of early floods, and attention should be paid to potential drought in the middle JRB.	Annual streamflow increased by ~14%, and the peak streamflow increased by more than 25%. The middle and lower JRB showed a 15% increase in streamflow.	Much more attention should be given to the flood control capacity of the reservoir to fully exploit the advantages of the group of reservoirs.
LA	The peak streamflow value appeared one month earlier, and the precipitation distribution was more uneven. The upper and middle JRB showed a more than 10% decrease in streamflow, whereas the lower part showed a more than 10% increase.	Reservoir managers should be cautious of early floods and water supply projects, e.g., the South-to-North Water Transfer West Route Project, may be affected in the future.	Annual streamflow showed a more than 14% increase, and the streamflow in summer showed an increase of ~20%. The peak streamflow showed a more than 15% increase, and streamflow in the lower JRB was 25% greater.	Reservoir managers should beware of the increased risk of flood disasters as well as other related disasters, including landslides.
pIOD	Annual streamflow decreased by ~9%, and the streamflow in autumn showed a more than 10% decrease. The extreme streamflow decreased by ~20%, except for the upper JRB, and streamflow in the other sub-basins showed a more than 10% decrease.	Water resource managers should be cautious of the increased risk of drought disasters, as reservoir functions such as hydropower generation and water supply may be affected. Additionally, reservoir managers should take advanced measures such as reservoir recharge to ensure that the reservoir is always full.	The streamflow in summer showed a 15% increase, and the streamflow in the lower JRB showed a 10% increase.	Strategies to cope with floods in the lower JRB during summer should be carefully implemented.

Table 2. *Cont.*

| | Developing Years | | Decaying Years | |
	Streamflow Characteristics Relative to Neutral Years	Suggestions	Streamflow Characteristics Relative to Neutral Years	Suggestion
nIOD	Annual streamflow decreased by ~7%, and summer streamflow showed a more than 10% decrease. Additionally, the streamflow in the lower JRB showed a decrease of more than 20%.	The lower JRB may be affected by serious drought. Therefore, reservoir managers should recognize that reservoir functions such as hydropower generation, and water allocation may be affected.	Summer streamflow showed a 14% increase, and the extreme value of the streamflow increased by more than 20%. Additionally, streamflow in the lower JRB showed a more than 15%increase.	Similar to pIOD; however, the extent of the streamflow increase would be higher.
EI/pIOD	Annual streamflow showed a more than 10% decrease, and summer and autumn streamflow showed a more than 10% decrease. Additionally, the streamflow in all the sub-basins decreased by ~10%.	Similar to pIOD; however, the impact of this combination could be more severe than that of pIOD only.	Similar to neutral years.	/
LA/pIOD	Annual streamflow showed a more than 10% decrease, and summer and autumn streamflow decreased by ~17%. Streamflow in the middle and lower JRB as well as the Yalong sub-basin decreased by more than 10%.	Severe drought may attack the JRB, resulting in a decrease in streamflow. This can bring new challenges concerning meeting all types of water needs, including irrigation as well as industrial and domestic uses. Reservoir managers can apply the optimal allocation of water resources. Additionally, reservoir operation can be used to deal with shortages.	Annual streamflow showed a more than 10% increase, and the extreme streamflow value showed a more than 20% increase. Additionally, the summer streamflow increased by 20%, and streamflow in the upper JRB showed a more than 50% increase.	In summer, severe flood events may occur, especially in the upper JRB.
LA/nIOD	Annual streamflow increased by ~7%, and autumn streamflow showed a more than 10% increase. Additionally, streamflow in the upper JRB showed a more than 20% increase.	Attention should be given to flood control in autumn, especially in the upper JRB.	Summer streamflow increased by 10%, and streamflow in the upper JRB showed a more than 20%increase.	In summer, much more attention should be paid to flood control in the upper JRB

5. Conclusions

Despite several studies on the impacts of ENSO or IOD events on streamflow in the Yangtze River, this study is the first to investigate the comprehensive impact of ENSO and IOD events on streamflow in the JRB, including annual and seasonal average streamflow, spatial and temporal patterns of streamflow, and extreme streamflow conditions. The results showed that both ENSO and IOD events affect annual and seasonal streamflow in the JRB, and their impacts differ in different phases. In developing years, the impact of pure IOD events on annual streamflow was twice that of pure ENSO events, whereas the opposite was true in decaying years. Compared with pure ENSO and IOD events, their simultaneous occurrence, especially the simultaneous occurrence of La Niña and pIOD events, resulted in greater differences in JJA0, SON0, and JJA1 in most cases.

The different phases of the climate indices had different impacts on the temporal and spatial patterns of streamflow in the JRB. In developing years, pure IOD events appeared to reduce the peak streamflow value, whereas pure ENSO events resulted in an earlier peak value relative to neutral years. However, in decaying years, the occurrence of pure ENSO events resulted in an increase in the peak streamflow value (up to 20%) in September, and the impact of the simultaneous occurrence of La Niña and pIOD events was even greater. In addition, in developing years, the impact of the climatic indices on streamflow in the SRJRB contrasted with that in the other sub-basins in most cases. In decaying years, the simultaneous occurrence of ENSO and IOD events had the most significant impact on streamflow in the SRJRB relative to the other sub-basins.

ENSO and IOD events had different impacts on the streamflow maxima/minima, whereas the 1-day/3-day/7-day minimal were different in most cases. The greatest impact on the streamflow maxima was observed at Zhimenda Station owing to the simultaneous occurrence of La Niña and pIOD events, which resulted in a 50% difference in the maxima streamflow relative to neutral years. In most cases, the impact on the streamflow minima was less than 10% in both developing and decaying years, except at Zhimenda Station, which indicates that the source region of the Yangtze River is more sensitive to ENSO/IOD events.

In most previous studies, the impact of the ENSO or IOD was investigated separately, with a focus on precipitation and annual streamflow. This study indicated that the combination of ENSO and IOD may have a greater impact on streamflow than pure events and that the streamflow maxima is more sensitive to the SSTA than annual or seasonal streamflow. Thus, the impact of ENSO on precipitation or streamflow in the JRB, along with other highly relevant climate indices such as IOD, could provide new insights into more effective water management in other basins for power generation and agriculture. Moreover, analyzing the impact of the ENSO or other climate indices in different phases can result in different insights for water resource managers. For example, when ENSO and IOD occur simultaneously, managers need to pay more attention to drought prevention if it occurs in a developing year and to flood prevention if it occurs in a declining year. However, this study is only a preliminary analysis of the impact of ENSO and IOD events on streamflow, which is mainly based on remote correlation analysis and statistics of different streamflow characteristics under different ENSO and IOD scenarios. The mechanism by which ENSO and IOD events influence streamflow in the JRB via large-scale atmospheric circulation changes needs further investigation. In this study, ENSO and IOD events are considered two independent events, and further research is needed to investigate whether there is a correlation between these two SST anomalous events. In addition, studies on water resources management are based on practical experience and need to be quantified by models, such as multi-objective reservoir operation models.

Conflicts of Interest: The authors have no conflict of interest to declare that are relevant to the content of this article.

References

1. Zhang, Q. The South-to-North Water Transfer Project of China: Environmental Implications and Monitoring Strategy1. *J. Am. Water Res. Assoc.* **2009**, *451*, 238–1247. [CrossRef]
2. Ni, X.K.; Dong, Z.C.; Xie, W.; Jia, W.H.; Duan, C.G.; Yao, H.Y. Research on the Multi-Objective Cooperative Competition Mechanism of Jinsha River Downstream Cascade Reservoirs during the Flood Season Based on Optimized NSGA-III. *Water* **2019**, *11*, 849. [CrossRef]
3. Jia, W.; Dong, Z.; Duan, C.; Ni, X.; Zhu, Z. Ecological reservoir operation based on DFM and improved PA-DDS algorithm: A case study in Jinsha river, China. *Hum. Ecol. Risk Assess. Int. J.* **2020**, *26*, 1723–1741. [CrossRef]
4. Fu, G.; Charles, S.P.; Viney, N.R.; Chen, S.; Wu, J.Q. Impacts of climate variability on stream-flow in the Yellow River. *Hydrol. Process.* **2007**, *21*, 3431–3439. [CrossRef]
5. Ropelewski, C.F.; Halpert, M.S.J.M.W.R. Global and Regional Scale Precipitation Patterns Associated with the El Niño/Southern Oscillation. *Mon. Weather Rev.* **1987**, *115*, 1606–1626. [CrossRef]
6. Wang, B.; Wu, R.; Fu, X. Pacific–East Asian Teleconnection: How Does ENSO Affect East Asian Climate? *J. Clim.* **2000**, *13*, 1517–1536. [CrossRef]
7. Timmermann, A.; An, S.-I.; Kug, J.-S.; Jin, F.-F.; Cai, W.; Capotondi, A.; Cobb, K.M.; Lengaigne, M.; McPhaden, M.J.; Stuecker, M.F.; et al. El Niño–Southern Oscillation complexity. *Nature* **2018**, *559*, 535–545. [CrossRef]
8. Wei, J.; Wang, W.; Shao, Q.; Rong, Y.; Xing, W.; Liu, C. Influence of mature El Niño-Southern Oscillation phase on seasonal precipitation and streamflow in the Yangtze River Basin, China. *Int. J. Climatol.* **2019**, *40*, 3885–3905. [CrossRef]
9. Chongyin, L. Interaction between anomalous winter monsoon in East Asia and El Nino events. *Adv. Atmos. Sci.* **1990**, *7*, 36–46. [CrossRef]
10. Wu, R.; Hu, Z.-Z.; Kirtman, B.P. Evolution of ENSO-Related Rainfall Anomalies in East Asia. *J. Clim.* **2003**, *16*, 3742–3758. [CrossRef]
11. Feng, J.; Chen, W.; Tam, C.Y.; Zhou, W. Different impacts of El Niño and El Niño Modoki on China rainfall in the decaying phases. *Int. J. Climatol.* **2011**, *31*, 2091–2101. [CrossRef]
12. Zhang, W.; Jin, F.-F.; Turner, A. Increasing autumn drought over southern China associated with ENSO regime shift. *Geophys. Res. Lett.* **2014**, *41*, 4020–4026. [CrossRef]
13. Zhou, L.-T.; Wu, R. Respective impacts of the East Asian winter monsoon and ENSO on winter rainfall in China. *J. Geophys. Res. Atmos.* **2010**, *115*. [CrossRef]
14. Živković, T.; Rypdal, K. ENSO dynamics: Low-dimensional-chaotic or stochastic? *J. Geophys. Res. Atmos.* **2013**, *118*, 2161–2168. [CrossRef]
15. Torrence, C.; Webster, P.J. Interdecadal Changes in the ENSO–Monsoon System. *J. Clim.* **1999**, *12*, 2679–2690. [CrossRef]
16. Saji, N.H.; Goswami, B.N.; Vinayachandran, P.N.; Yamagata, T. A dipole mode in the tropical Indian Ocean. *Nature* **1999**, *401*, 360–363. [CrossRef] [PubMed]
17. Guan, Z.; Yamagata, T. The unusual summer of 1994 in East Asia: IOD teleconnections. *Geophys. Res. Lett.* **2003**, *30*. [CrossRef]
18. Yang, J.; Liu, Q.; Xie, S.-P.; Liu, Z.; Wu, L. Impact of the Indian Ocean SST basin mode on the Asian summer monsoon. *Geophys. Res. Lett.* **2007**, *34*. [CrossRef]
19. Weng, H.; Wu, G.; Liu, Y.; Behera, S.K.; Yamagata, T. Anomalous summer climate in China influenced by the tropical Indo-Pacific Oceans. *Clim. Dyn.* **2011**, *36*, 769–782. [CrossRef]
20. Qiu, Y.; Cai, W.; Guo, X.; Ng, B. The asymmetric influence of the positive and negative IOD events on China's rainfall. *Sci. Rep.* **2014**, *4*, 4943. [CrossRef]
21. Zheng, J.; Liu, Q.; Wang, C.; Zheng, X.-T. Impact of Heating Anomalies Associated with Rainfall Variations over the Indo-Western Pacific on Asian Atmospheric Circulation in Winter. *Clim. Dyn.* **2013**, *40*, 2023–2033. [CrossRef]
22. Xiao, M.; Zhang, Q.; Singh, V.P. Influences of ENSO, NAO, IOD and PDO on seasonal precipitation regimes in the Yangtze River basin, China. *Int. J. Climatol.* **2015**, *35*, 3556–3567. [CrossRef]
23. Xiao, M.; Zhang, Q.; Singh, V.P. Spatiotemporal variations of extreme precipitation regimes during 1961–2010 and possible teleconnections with climate indices across China. *Int, J. Climatol.* **2017**, *37*, 468–479. [CrossRef]
24. Gao, T.; Wang, H.J.; Zhou, T. Changes of extreme precipitation and nonlinear influence of climate variables over monsoon region in China. *Atmos. Res.* **2017**, *197*, 379–389. [CrossRef]
25. Xu, K.; Zhu, C.; Wang, W. The cooperative impacts of the El Niño–Southern Oscillation and the Indian Ocean Dipole on the interannual variability of autumn rainfall in China. *Int. J. Climatol.* **2016**, *36*, 1987–1999. [CrossRef]
26. Pillai, P.A.; Ramu, D.A.; Nair, R.C. Recent changes in the major modes of Asian summer monsoon rainfall: Influence of ENSO-IOD relationship. *Theor. Appl. Climatol.* **2021**, *143*, 869–881. [CrossRef]
27. Cao, Q.; Hao, Z.; Yuan, F.; Su, Z.; Berndtsson, R. ENSO Influence on Rainy Season Precipitation over the Yangtze River Basin. *Water* **2017**, *9*, 469. [CrossRef]
28. Cao, Q.; Hao, Z.C.; Yuan, F.F.; Su, Z.K.; Berndtsson, R.; Hao, J.; Nyima, T. Impact of ENSO regimes on developing- and decaying-phase precipitation during rainy season in China. *Hydrol. Earth Syst. Sci.* **2017**, *21*, 5415–5426. [CrossRef]

29. Kumar, R.; Samaniego, L.; Attinger, S. The effects of spatial discretization and model parameterization on the prediction of extreme runoff characteristics. *J. Hydrol.* **2010**, *392*, 54–69. [CrossRef]

30. Ding, Z.; Fang, G.; Wen, X.; Tan, Q.; Huang, X.; Lei, X.; Yu, T.; Jin, Q. A novel operation chart for cascade hydropower system to alleviate ecological degradation in hydrological extremes. *Ecol. Model.* **2018**, *384*, 10–22. [CrossRef]

31. Hong, C.-C.; Lu, M.-M.; Kanamitsu, M. Temporal and spatial characteristics of positive and negative Indian Ocean dipole with and without ENSO. *J. Geophys. Res.* **2008**, *113*. [CrossRef]

32. Wang, S.; Zhang, X.; Liu, Z.; Wang, D. Trend Analysis of Precipitation in the Jinsha River Basin in China. *J. Hydrometeor* **2013**, *14*, 290–303. [CrossRef]

33. Li, D.; Lu, X.X.; Yang, X.; Chen, L.; Lin, L. Sediment load responses to climate variation and cascade reservoirs in the Yangtze River: A case study of the Jinsha River. *Geomorphology* **2018**, *322*, 41–52. [CrossRef]

34. Zhang, Q.; Xu, C.-y.; Jiang, T.; Wu, Y. Possible influence of ENSO on annual maximum streamflow of the Yangtze River, China. *J. Hydrol.* **2007**, *333*, 265–274. [CrossRef]

35. Dong, Q.; Fang, D.; Zuo, J.; Wang, Y. Hydrological alteration of the upper Yangtze River and its possible links with large-scale climate indices. *Hydrol. Res.* **2019**, *50*, 1120–1137. [CrossRef]

36. Grinsted, A.; Moore, J.C.; Jevrejeva, S. Application of the cross wavelet transform and wavelet coherence to geophysical time series. *Nonlinear Process. Geophys.* **2004**, *11*, 561–566. [CrossRef]

37. Jarvis, C.; Darbyshire, R.; Eckard, R.; Goodwin, I.; Barlow, E. Influence of El Niño-Southern Oscillation and the Indian Ocean Dipole on winegrape maturity in Australia. *Agric. For. Meteorol.* **2018**, *248*, 502–510. [CrossRef]

38. Ashok, K.; Guan, Z.; Saji, N.H.; Yamagata, T. Individual and Combined Influences of ENSO and the Indian Ocean Dipole on the Indian Summer Monsoon. *J. Clim.* **2004**, *17*, 3141–3155. [CrossRef]

39. Li, C.; Zhao, T. Seasonal Responses of Precipitation in China to El Niño and Positive Indian Ocean Dipole Modes. *Atmosphere* **2019**, *10*, 372. [CrossRef]

40. Kim, H.M.; Webster, P.J.; Curry, J.A. Impact of Shifting Patterns of Pacific Ocean Warming on North Atlantic Tropical Cyclones. *Science* **2009**, *325*, 77–80. [CrossRef]

41. Ahern, M.; Kovats, R.S.; Wilkinson, P.; Few, R.; Matthies, F. Global Health Impacts of Floods: Epidemiologic Evidence. *Epidemiol. Rev. Epidemiol. Rev.* **2005**, *27*, 36–46. [CrossRef] [PubMed]

42. Guo, A.; Chang, J.; Liu, D.; Wang, Y.; Huang, Q.; Li, Y. Variations in the precipitation–runoff relationship of the Weihe River Basin. *Hydrol. Res.* **2016**, *48*, 295–310. [CrossRef]

43. Sankarasubramanian, A.; Vogel, R.M.; Limbrunner, J.F. Climate elasticity of streamflow in the United States. *Water Resour. Res.* **2001**, *37*, 1771–1781. [CrossRef]

44. Tong, J.; Qiang, Z.; Deming, Z.; Yijin, W. Yangtze floods and droughts (China) and teleconnections with ENSO activities (1470–2003). *Quat. Int.* **2006**, *144*, 29–37. [CrossRef]

45. Ouyang, R.; Liu, W.; Fu, G.; Liu, C.; Hu, L.; Wang, H. Linkages between ENSO/PDO signals and precipitation, streamflow in China during the last 100 years. *Hydrol. Earth Syst. Sci.* **2014**, *18*, 3651–3661. [CrossRef]

46. Cai, W.; Cai, W.; Rensch, P.V.; Cowan, T.; Hendon, H.H. An Asymmetry in the IOD and ENSO Teleconnection Pathway and Its Impact on Australian Climate. *J. Clim.* **2012**, *25*, 6318–6329. [CrossRef]

47. Yuan, Y.; Yang, H.; Zhou, W.; Li, C. Influences of the Indian Ocean dipole on the Asian summer monsoon in the following year. *Int. J. Climatol.* **2008**, *28*, 1849–1859. [CrossRef]

48. Meyers, G.; McIntosh, P.; Pigot, L.; Pook, M. The years of El Niño, La Niña and interactions with the tropical Indian Ocean. *J. Clim.* **2007**, *20*, 2872–2880. [CrossRef]

49. Chang, C.-P.; Zhang, Y.; Li, T. Interannual and Inter.rdecadal Variations of the East Asian Summer Monsoon and Tropical Pacific SSTs. Part I: Roles of the Subtropical Ridge. *J. Clim.* **2000**, *13*, 4310–4325. [CrossRef]

50. Wan, S.; Hu, Y.; You, Z.; Kang, J.; Zhu, J. Extreme monthly precipitation pattern in China and its dependence on Southern Oscillation. *Int. J. Climatol.* **2013**, *33*, 806–814. [CrossRef]

51. Sun, X.; Renard, B.; Thyer, M.; Westra, S.; Lang, M. A global analysis of the asymmetric effect of ENSO on extreme precipitation. *J. Hydrol.* **2015**, *530*, 51–65. [CrossRef]

52. Cheng, Q.; Gao, L.; Zuo, X.; Zhong, F. Statistical analyses of spatial and temporal variabilities in total, daytime, and nighttime precipitation indices and of extreme dry/wet association with large-scale circulations of Southwest China 1961–2016. *Atmos. Res.* **2019**, *219*, 166–182. [CrossRef]

53. Szemis, J.M.; Maier, H.R.; Dandy, G.C. An adaptive ant colony optimization framework for scheduling environmental flow management alternatives under varied environmental water availability conditions. *Water Resour. Res.* **2014**, *50*, 7606–7625. [CrossRef]

54. Huang, K.; Ye, L.; Chen, L.; Wang, Q.; Ling, D.; Zhou, J.; Signh, V.P.; Huang, M.; Zhang, J. Risk analysis of flood control reservoir operation considering multiple uncertainties. *J. Hydrol.* **2018**, *565*, 672–684. [CrossRef]

55.   Lin, Q.; Wu, Z.; Singh, V.P.; Sadeghi, S.H.R.; He, H.; Lu, G. Correlation between hydrological drought, climatic factors, reservoir operation, and vegetation cover in the Xijiang Basin, South China. *J. Hydrol.* **2017**, *549*, 512–524. [CrossRef]